Hindawi Publishing Corporation
EURASIP Journal on Advances in Signal Processing
Volume 2008, Article ID 356267, 8 pages
doi:10.1155/2008/356267

Research Article

A Reconfigurable GNSS Acquisition Scheme for Time-Frequency Applications

Daniele Borio[1] and Letizia Lo Presti[2]

[1] *Department of Geomatics Engineering, University of Calgary, 2500 University Dr. NW, Calgary, AB, Canada T2N 1N4*
[2] *Dipartimento di Elettronica, Politecnico di Torino, Corso Duca degli Abruzzi 24, 10129 Torino, Italy*

Correspondence should be addressed to Daniele Borio, daniele.borio@polito.it

Received 11 November 2007; Accepted 11 June 2008

Recommended by Sven Erik Nordholm

The extreme weakness of global navigation satellite system (GNSS) signals makes them vulnerable to almost every kind of interferences that, without adequate countermeasures, can heavily compromise the receiver performance. An effective solution is represented by time-frequency (TF) analysis that has proved to be able to detect and suppress a wide class of disturbing signals. However, high computational requirements have limited the diffusion of such techniques for GNSS applications. In this paper, we propose an effective solution for the efficient implementation of TF techniques on GNSS receivers. The solution is based on the key observation that the first block of a GNSS receiver, the acquisition stage, implicitly performs a sort of TF analysis. Thus, a slight modification in the traditional acquisition scheme enables the fast and efficient implementation of TF techniques for interference detection. The proposed method is suitable for different types of acquisition scheme and its effectiveness is proved by simulations and examples on real data.

1. INTRODUCTION

In the last few years, global navigation satellite systems (GNSS) are experiencing a considerable development, essentially boosted by the growing demand of services based on precise positioning. The augmented global positioning system (GPS), the Russian Glonass, and the new European and Chinese GNSSs, Galileo and Compass, will provide, in the near future, full earth coverage, allowing localization-based services everywhere and at anytime. On the other side, GNSS receivers will be required to operate in different and often adverse conditions such as indoor and in urban environments. In this context, future GNSS receivers will be also required to work in presence of strong interference and thus they will be equipped with specific antijamming units. However, due to its weakness, the GNSS signal is subject to interferences that are extremely different in terms of time and frequency characteristics [1]. Thus the design of a general detector/mitigator, able to efficiently deal with different kinds of interference, is a complex problem.

A solution is represented by time-frequency (TF) analysis [2], that allows to detect and efficiently remove a great variety of disturbing signals. Time-frequency representations (TFRs) map a one-dimensional signal of time, $x(t)$, into a two-dimensional function of time and frequency, $T_x(t, f)$. In this way, the signal is characterized over a time-frequency plane yielding to a potentially more revealing picture of the temporal localization of the signals spectral components.

In the past, a great interest has been devoted to TF excision techniques in the context of direct-sequence spread spectrum (DSSS) communications [3–8]. This interest is justified by the fact that the power of DSSS signals is spread over a bandwidth that is much wider than the original information bandwidth. As a result, DSSS signals present power spectral densities that can be completely hidden under the noise floor and, consequently, they only marginally impact the interference detection/estimation on the TF plane.

In the context of GNSS, the use of TF analysis has been limited by the heavy computational load required by these techniques. The length of spreading sequences, up to several thousands of symbols [9, 10], and the consequent memory and computational load, along with stringent real-time constraints, often leave an extremely limited amount

of computational resources for additional units, for example for interference detection and mitigation. Thus other techniques, less computationally demanding, such as notch filtering [11] and frequency excision [12], have been preferred to TF analysis. However, the use of these detection/mitigation techniques is often confined to a specific class of disturbing signals resulting in a completely ineffective processing for those interferences presenting time/frequency characteristics different from the ones for which the algorithms were designed.

In the literature, some TF algorithms have been specifically developed for GNSS applications. However, the implementation aspects are often only marginally discussed. Reference [13] proposes a TF detection/excision algorithm for GPS receivers, based on the Wigner-Ville distribution. Although the method is promising, [13] does not discuss any implementation issue as well as the computational requirements of the proposed method.

In [14], an excision algorithm based on the short time Fourier transform (STFT) and the spectrogram is proposed. The method is implemented by exploiting the structure of the FFT-based acquisition scheme [15] that is however suitable only for those receivers that evaluate correlations using the FFT. Moreover, the method from [14] does not allow the use of analysis windows different from the rectangular one. The size of the analysis windows is also fixed and corresponds to the FFT size, potentially resulting in spectral leakage [16] and poor TFRs.

In this paper, a solution for efficiently implementing TF techniques in GNSS receivers is proposed. This solution is based on the key observation that the first block of a GNSS receiver, the acquisition stage, implicitly performs a sort of TF analysis. In the acquisition stage, the delay and the Doppler frequency of the GNSS signal are estimated exploiting the correlation properties of the pseudorandom noise (PRN) sequences used for spreading the transmitted signal. In this paper, we show that the evaluation of the search space for the delay and the Doppler frequency corresponds to the evaluation of a spectrogram, whose analysis window is adapted to the received signal. Thus the adoption of a different analysis window allows the detection/estimation of disturbing signals. Based on this principle, the method described in this paper proposes a slight modification of the basic acquisition scheme that allows a fast and efficient TF analysis for interference detection. The method reuses the resources already available for the acquisition stage and the analysis can be performed when the normal acquisition operations shut down or stand temporally idle. Thus, the major of contribution of this paper is the design of a reconfigurable acquisition scheme allowing TF applications. The proposed method is suitable for all acquisition schemes, such as the serial search [17] as well as parallel searches in time [15] and in frequency domains [18].

The paper is organized as follows. in Section 2, the model for the GNSS signal in presence of interference is introduced. The acquisition principles and the spectrogram are also reviewed highlighting the analogies between the two processes. In Section 3, the modified acquisition block for TF applications is discussed and adapted to the different acquisition schemes. In Section 4, a detection algorithm based on the modified acquisition block is proposed. Section 5 assesses the algorithm performance with both simulated and real data. Finally, Section 6 concludes the paper.

2. SIGNAL AND SYSTEM MODEL

The input of the acquisition block is generally an intermediate frequency (IF) digital signal obtained at the front-end output, which can be written in the form [9]

$$r[n] = r(nT_s) = \sum_{i=1}^{L_s} y_{\mathrm{IF},i}(nT_s) + N_{\mathrm{IF}}(nT_s), \tag{1}$$

where L_s is the number of satellites in view, T_s is the sampling interval, $N_{\mathrm{IF}}(nT_s)$ is a disturbing term and $y_{\mathrm{IF},i}(nT_s)$ are the samples of the signal

$$y_{\mathrm{IF},i}(t) = \sqrt{2C_i}c_i(t-\tau^a_{0,i})d_i(t-\tau^a_{0,i})\cdot\cos\left(2\pi\left(f_{\mathrm{IF}}+f^0_{d,i}\right)t+\varphi^0_i\right) \tag{2}$$

transmitted by the ith satellite and recovered by the front-end. C_i and $c_i(t-\tau^a_{0,i})$ are the received power and the spreading code of the ith satellite, $d_i(t-\tau^a_{0,i})$ represents the bit stream of the navigation message, f_{IF} is the receiver intermediate frequency (IF), and φ^0_i is a random phase. Both the code and the navigation message are delayed by $\tau^a_{0,i}$; $f^0_{d,i}$ is the Doppler shift of the ith satellite. In (1), the quantization effect has been neglected. In the following, the notation $x[n] = x(nT_s)$ will indicate a discrete-time sequence $x[n]$, obtained by sampling a continuous-time signal $x(t)$ with a sampling frequency $f_s = 1/T_s$.

The disturbing signal $N_{\mathrm{IF}}[n] = N_{\mathrm{IF}}(nT_s)$ can be expressed as

$$N_{\mathrm{IF}}[n] = I_{\mathrm{IF}}[n] + W_{\mathrm{IF}}[n], \tag{3}$$

where $I_{\mathrm{IF}}[n]$ is, in general, a nonstationary interference and $W_{\mathrm{IF}}[n]$ is a Gaussian noise whose spectral characteristics depend on the type of filtering and on the sampling and decimation strategy adopted at the front-end. A convenient choice is to sample the IF signal with a sampling frequency $f_s = 2B_{\mathrm{IF}}$, where B_{IF} is the front-end bandwidth. Before sampling, an antialiasing low-pass filter with bandwidth $f_s/2$ is generally applied. In this case, it is easily shown that the noise variance becomes

$$\sigma^2_{\mathrm{IF}} = E\{W^2_{\mathrm{IF}}(t)\} = E\{W^2_{\mathrm{IF}}(nT_s)\} = \frac{N_0 f_s}{2} = N_0 B_{\mathrm{IF}}, \tag{4}$$

where $N_0/2$ is the power spectral density of the IF noise. The autocorrelation function

$$R_{\mathrm{IF}}[m] = E\{W_{\mathrm{IF}}(nT_s)W_{\mathrm{IF}}((n+m)T_s)\} = \sigma^2_{\mathrm{IF}}\delta[m] \tag{5}$$

implies that the discrete-time random process $W_{\mathrm{IF}}[n]$ is a classical i.i.d. (independent and identically distributed) random process, or a white sequence.

The interference $I_{\mathrm{IF}}[n]$ can assume several time-frequency characteristics [1] that have to be estimated, for

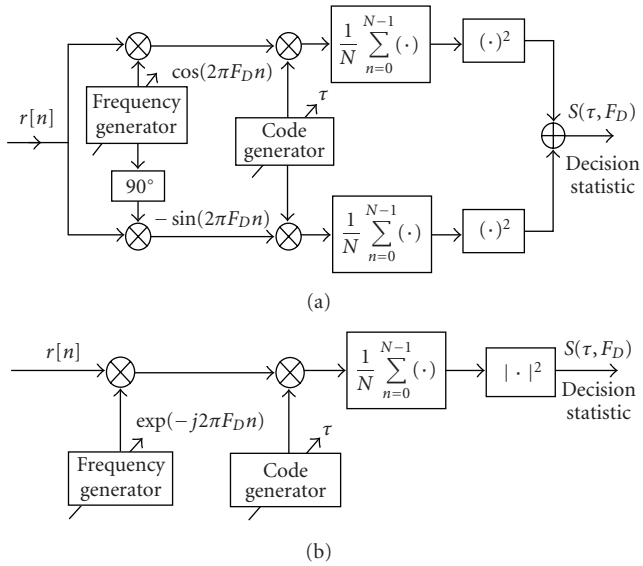

Figure 1: (a) Scheme of a GNSS acquisition block using coherent integrations only. The low-pass filters after the cosine/sine multiplications have been omitted, since the coherent integrations block already acts like a low-pass filter. (b) Equivalent acquisition scheme in terms of complex signals.

example, by means of TF techniques. The interference mean power is defined as the variance of the disturbing signal $I_{\mathrm{IF}}[n]$:

$$J[n] = \mathrm{Var}\{I_{\mathrm{IF}}[n]\}, \tag{6}$$

that can be, in general, time-varying. The jammer-to-noise ratio is defined as

$$\frac{J[n]}{N} = \frac{J[n]}{\sigma_{\mathrm{IF}}^2} = \frac{J[n]}{N_0 B_{\mathrm{IF}}}. \tag{7}$$

As a result of code orthogonality, the different GNSS codes are analyzed separately by the acquisition block and thus the case of a single satellite is considered hereinafter; thus the resulting signal is

$$\begin{aligned} r[n] = {} & \sqrt{2C}c[n-\tau_0]d[n-\tau_0]\cos(2\pi F_{D,0}n + \varphi^0) \\ & + I_{\mathrm{IF}}[n] + W_{\mathrm{IF}}[n], \end{aligned} \tag{8}$$

where $F_{D,0} = (f_{\mathrm{IF}} + f_d^0)T_s$ and $\tau_0 = \tau_0^a/T_s$.

2.1. The acquisition process

In Figure 1(a), the scheme of a conventional acquisition system [10] is shown: a local replica of the GNSS code, delayed by τ, and two orthogonal sinusoids at the frequency $F_D = (f_{\mathrm{IF}} + f_d)T_s$ are generated and multiplied by the received signal $r[n]$. The resulting signals are coherently integrated leading to the in-phase and quadrature components $S_I(\tau, F_D)$ and $S_Q(\tau, F_D)$. N is the number of samples used for the integration process and NT_s is the coherent integration time.

$S_I(\tau, F_D)$ and $S_Q(\tau, F_D)$ are then squared and summed, removing the dependence from the input signal phase φ^0. In this way, a bidimensional function $S(\tau, F_D)$ is obtained. $S(\tau, F_D)$ is evaluated for a finite and discrete set of values of τ and F_D of the type

$$\tau = \tau_b + m\Delta\tau, \quad m = 0, 1, \ldots, H-1, \tag{9}$$

$$F_D = F_b + l\Delta f, \quad l = 0, 1, \ldots, K-1. \tag{10}$$

The values of the parameters τ_b, F_b, $\Delta\tau$, Δf, H, and K depend on various factors, whose analysis is out of the scope of this paper. The grid of values of τ and F_D represents the so-called search space, which is a plane, containing $N_t = H \times K$ cells, H delay bins, and K Doppler bins.

In Figure 1(b), the traditional acquisition scheme has been restated in terms of complex signals: the multiplication by the two orthogonal sinusoids is interpreted as a complex modulation whereas the sum of the squared in-phase and quadrature components is represented as a complex square modulus. In this way, $S(\tau, F_D)$ can be expressed as

$$S(\tau, F_D) = \left| \frac{1}{N} \sum_{n=0}^{N-1} r[n]c[n-\tau] \exp\{-j2\pi F_D n\} \right|^2. \tag{11}$$

2.2. The spectrogram

The magnitude squared of the Fourier transform is the classical method used to represent the frequency information or spectrum of a stationary signal. However, the classical Fourier transform results completely ineffective when dealing with nonstationary signals, since the time variation of frequency information is averaged over the whole signal duration. A solution is represented by the STFT [2, 19] which is evaluated by applying a suitable windowing function to the original signal and evaluating the conventional Fourier transform of the resulting finite length sequence. The STFT of a finite-length discrete signal $r[n]$ is given by

$$\mathrm{STFT}(\tau, f) = \sum_{n=0}^{N-1} r[n]w[n-\tau] \exp\{-j2\pi f n\}, \tag{12}$$

where $w[\tau]$ is the windowing function of duration T_w. Although the summation in (12) is performed over the whole signal duration, the windowing function $w[\tau]$ captures only T_w samples of signal $r[n]$ for each value of τ. $r[n]$ is assumed stationary over the short time interval T_w. Using this technique, an approximation to the spectral content at the midpoint of the window interval can be achieved by computing $S_w(\tau, f) = |\mathrm{STFT}(\tau, f)|^2$ that is the discrete spectrogram [2, 19]:

$$S_w(\tau, f) = \left| \sum_{n=0}^{N-1} r[n]w[n-\tau] \exp\{-j2\pi f n\} \right|^2. \tag{13}$$

The TF resolution of the STFT and of the spectrogram is strictly related to the window length: large T_w allows a good frequency resolution at the expense of the time characterization. Conversely, short analysis windows guarantee better time resolutions. For this reason, different analysis windows have to be tested in order to provide a good TF characterization of the signal under analysis [20].

By comparing (11) and (13), it clearly emerges that the decision variable for the acquisition block is a spectrogram scaled by the factor $1/N^2$ and with

$$w[\tau] = c[\tau] \tag{14}$$

that is with the analysis window adapted to the GNSS signal. Since $S(\tau, F_D)$ and $S_w(\tau, f)$ have basically the same structure, the same functional blocks used for evaluating $S(\tau, F_D)$ can be employed for determining $S_w(\tau, f)$. Thus, by replacing the local code with an appropriate analysis window and by extending the Doppler frequency interval in order to include all the frequency bands possibly affected by interfering signals, the acquisition block can be easily employed for TF applications.

3. THE MODIFIED ACQUISITION BLOCK

In the GNSS literature [9, 18, 21], different acquisition schemes are employed for determining a first, rough estimation of the code delay and Doppler frequency of the signal emitted by the satellite under analysis. These methods can be classified in three main classes:

(i) the classical serial search acquisition scheme [17, 22] that evaluates the search space cell by cell, subsequently testing the different values of code delay and Doppler shift;

(ii) the frequency domain FFT acquisition scheme [18], that exploits the fast Fourier transform (FFT) to evaluate all the Doppler frequencies in parallel. In this scheme, an integrate and dump (I&D) block can be used in order to reduce the frequency points to be evaluated by the FFT. The use of the FFT comports the analysis of frequency points outside the Doppler range;

(iii) the time domain FFT acquisition scheme [15], that uses the FFT to compute fast code circular convolution.

In this section, those three acquisition schemes are adapted in order to allow TF frequency applications. As highlighted in the previous section, the main differences between the decision variable(11) and the spectrogram (13) consist in fact of the following:

(i) the set of Doppler frequencies (10), searched for during the acquisition process, is usually limited to a few kHz around the receiver intermediate frequency, whereas the spectrogram needs to be evaluated for a wider range of frequencies;

(ii) the spectrogram and the decision variable $S(\tau, F_D)$ employ two different analysis windows.

Thus in order to reuse the acquisition computational resources for TF applications, these two differences have to be overcome. This can be easily achieved by introducing a window generator able to produce an analysis window for the TF analysis. The window generator can be either a memory bank or a digital device producing signals used as analysis window. Different analysis windows [16] can be stored in the memory bank and different window lengths can be obtained by means of downsampling: in the memory bank the full length version of an analysis window is stocked; when a shorter window is needed to increase the spectrogram time resolution, a new window is produced by downsampling the original one and adding the corresponding number of zeros. The simplest digital device producing analysis windows can be a generator of the signal

$$w[n] = \begin{cases} 1, & \text{for } n = 0, 1, \ldots, T_w - 1, \\ 0, & \text{for } n = T_w, \ldots, N - 1, \end{cases} \tag{15}$$

where T_w and N are the window and the local code length, respectively. Notice that varying the window length, the time-frequency resolution changes and different window lengths can be suitable for different kinds of interference. The window signal $w[n]$ should have the same length of the received signal $r[n]$ and of the local code $c[n]$, since the correlation is usually evaluated by multiplying two signals of the same length and integrating the result. A selector is used to switch from the normal acquisition mode to the TF one: in this way the local code $c[n]$ is substituted by the signal $w[n]$.

The delay τ, used to progressively shift the window analysis in (13), can assume values that are not in the set usually used for the search space computation. In particular, the step, $\Delta\tau$, used to explore all possible delay values (9) can be greater than T_s, the sampling interval. This allows faster computations and produces downsampled versions of the spectrogram that can be used for preliminary analysis.

The frequency range (10) can be extended by changing the initial frequency F_b, the frequency step Δf, and the number of frequency bins K. This can be achieved by adopting a frequency generator specifically designed for exploring a wider range of frequencies. The choice of increasing the number of Doppler bins comports a greater computational load whereas a too large frequency step Δf can result in a spectrogram poorly represented along the frequency dimension. For this reason, a compromise between frequency representation and computational load can be reached by changing both the Doppler step and the number of frequency bins.

In Figures 2, 3, and 4, the traditional acquisition schemes have been modified, introducing a window generator and an alternative frequency generator, allowing the evaluation of the spectrogram. It can be noted that the parallel acquisition scheme in frequency domain does not require an alternative frequency generator, since the use of the FFT for exploring the Doppler dimension already allows to analyze frequency points outside the Doppler range. In this case, the range of frequency under analysis depends on L, the number of points integrated by the I&D block.

4. TIME-FREQUENCY DETECTOR

GNSS acquisition is essentially a detection procedure used for establishing the presence or the absence of a signal

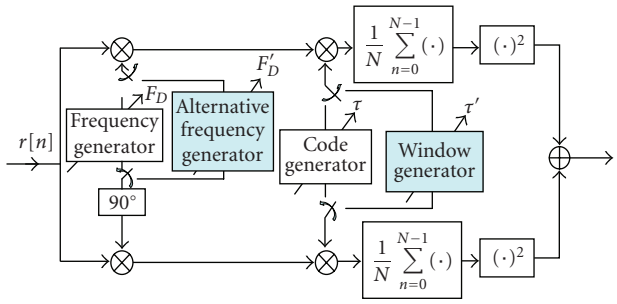

Figure 2: Modified serial search acquisition. The traditional serial search acquisition scheme has been modified in order to explore a wider range of Doppler frequencies and to allow the use of specific analysis windows for TF applications.

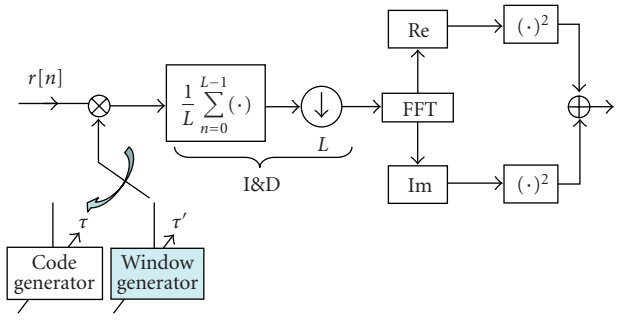

Figure 3: Modified parallel acquisition in frequency domain. The parallel acquisition scheme in frequency domain has been modified allowing the use of specific analysis windows for TF applications.

emitted by a specific satellite. Similarly, one of the main goals of the modified acquisition schemes proposed in the previous section is to detect the presence of disturbing signals. In traditional acquisition, the presence of the useful signal is declared when the decision statistic (11) passes a fixed threshold. This threshold is generally chosen in order to guarantee a certain false alarm probability, that is the probability that the decision statistic (11) leads to a detection when the signal is absent or not correctly aligned, either in time or in frequency. The proposed algorithm considers interference in the same way traditional acquisition schemes consider useful GNSS signals, where the analysis window is the "local code" that matches the interference TF characteristics. Thus the interfering signal can be detected by means of a threshold that is fixed according to the interference false alarm probability that is the probability that the spectrogram (13) leads to an interference detection in absence of disturbing signals.

When the interference signal is absent, the input signal (8) becomes

$$r[n] = \sqrt{2C}c[n-\tau_0]d[n-\tau_0]\cos(2\pi F_{D,0}n + \varphi^0) + W_{IF}[n]. \tag{16}$$

Moreover, the useful GNSS signal when the despreading process is not correctly performed is generally negligible with respect to the noise component and thus the signal that

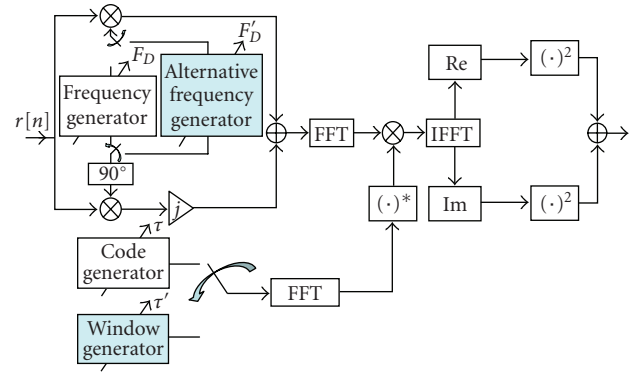

Figure 4: Modified parallel acquisition scheme in time domain. The parallel acquisition scheme in time domain has been modified in order to explore a wider range of Doppler frequencies and to allow the use of specific analysis windows for TF applications.

enters the modified acquisition block for TF applications can be effectively approximated as [9]

$$r[n] \approx W_{\text{IF}}[n]. \tag{17}$$

In this way, $r[n]$ can by considered as a white Gaussian process with zero mean and variance $\sigma^2_{\text{IF}} = N_0 B_{\text{IF}}$. Under this condition, the STFT (12), for each value of τ and f, is a zero mean Gaussian process with the variance

$$\begin{aligned}
&\text{Var}\{\text{STFT}(\tau, f)\} \\
&= E\{\text{STFT}(\tau, f)\text{STFT}(\tau, f)^*\} \\
&= \sum_{n=0}^{N-1}\sum_{k=0}^{N-1} E\{r[n]w[n-\tau]r[k]w^*[k-\tau]\exp\{-j2\pi f(n-k)\}\} \\
&= \sum_{n=0}^{N-1} E\{W^2_{\text{IF}}[n]\}|w[n-\tau]|^2 \\
&= \sigma^2_{\text{IF}}\sum_{n=0}^{N-1}|w[n-\tau]|^2 \;= E_w\sigma^2_{\text{IF}},
\end{aligned} \tag{18}$$

where E_w is the analysis window energy, that is independent from the delay applied to $w[n]$.

Furthermore, it is possible to show [23] that the square absolute value of a zero mean complex Gaussian random variable is a new random variable distributed according to an exponential law. More specifically, it is

$$S_w(\tau, f) \sim \text{Exp}\left(\frac{1}{\sigma^2_{\text{out}}}\right), \tag{19}$$

where $\sigma^2_{\text{out}} = E_w\sigma^2_{\text{IF}}$ is the variance of $\text{STFT}(\tau, f)$. The probability density function of $S_w(\tau, f)$ results in

$$f_w(s) = \frac{1}{\sigma^2_{\text{out}}}\exp\left\{-\frac{s}{\sigma^2_{\text{out}}}\right\} \tag{20}$$

and finally the interference false alarm probability equals

$$P_{\text{fa},I}(\beta) = \int_\beta^{+\infty} f_w(s)ds = \exp\left\{-\frac{\beta}{\sigma^2_{\text{out}}}\right\}, \tag{21}$$

Table 1: NordNav-R30 characteristics.

Sampling frequency	$f_s = 16.3676$ MHz
Intermediate frequency	$f_s = 4.1304$ MHz
Signal quantization	4 bits
Front-end filter bandwidth	≈ 2 MHz

where β is the threshold to be determined by fixing the false alarm probability and inverting (21). In this way, the threshold formula results in

$$\beta = -\sigma_{\text{out}}^2 \log P_{\text{fa},I}. \tag{22}$$

It has to be noted that when the modified acquisition process is used for evaluating the spectrogram, then (13) is scaled by a factor $1/N^2$, thus the threshold (22) has to be scaled by the same factor:

$$\beta' = -\frac{E_w \sigma_{\text{IF}}^2}{N^2} \log P_{\text{fa},I}. \tag{23}$$

Equation (23) is very close to the expression for the threshold for the traditional acquisition, and thus the same structures used for the satellite detection can be directly used for the interfering monitoring.

5. REAL-DATA AND SIMULATION TEST

In order to prove the effectiveness of the proposed acquisition scheme, some examples based on simulated and real data are reported in this section.

5.1. Real data

Real data have been collected by using the NordNav-R30 front-end [24] that is characterized by the specifications reported in Table 1. Data collection has been extensively performed in two different sites: the so-called "colle della Maddalena" and the hill of the "Basilica di Superga". These sites are located on two different hills on the side of Torino (Italy). The first one is characterized by the presence of several antennas for the transmission of analog and digital TV signals, whereas the second one is in direct view of the colle della Maddalena antennas. Two different kinds of interference have been observed. In the proximity of the colle della Maddalena, the GPS signal was corrupted by a swept interference, whereas a strong continuous wave interference (CWI) has been observed on the hill of Superga.

In Figure 5, the spectrogram of the swept interference observed in proximity of the colle della Maddalena has been depicted. This spectrogram has been evaluated by employing the modified parallel acquisition scheme in time domain described in the previous section. The input signal has been, at first, downsampled by a factor of 4 reducing the sampling frequency to $f_s = 4.0919$ MHz. This operation reduces the computational load without effectively degrading the signal quality since the NordNav front-end is characterized by a bandwidth of about 2 MHz. The Doppler step has been set to 10 kHz and the number of Doppler bins was $K = 201$.

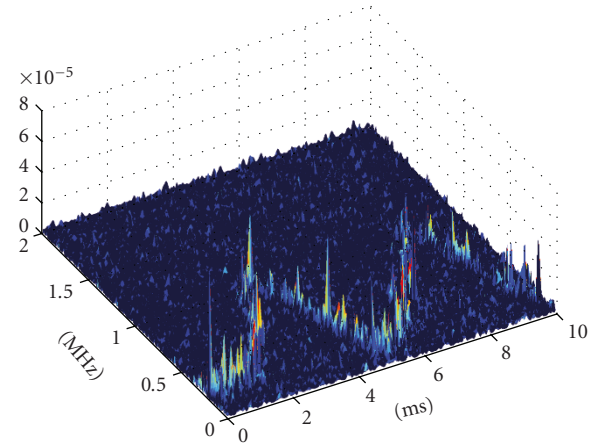

Figure 5: Spectrogram of a swept interference. The input signal has been collected by using the NordNav R30 front-end in the proximity of TV repeaters in Torino (Italy). The spectrogram has been evaluated by using the modified parallel acquisition scheme in time domain.

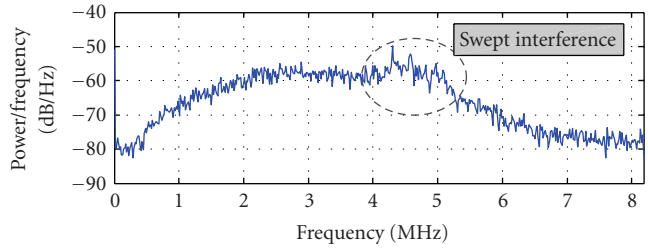

(a) Welch power spectral density estimate—original signal

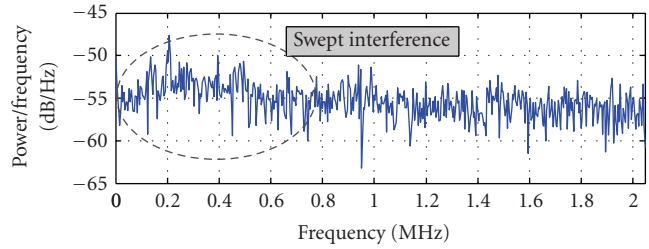

(b) Welch power spectral density estimate—downsampled signal

Figure 6: Power spectral density estimates of the input signal used for the evaluation of the spectrogram in Figure 5. (a) PSD of the original signal, sampling frequency $f_s = 16.3676$ MHz. (b) PSD of the downsampled signal, sampling frequency $f_s = 4.0919$ MHz.

A Hamming window of duration $T_w = N/10$ was employed. The analysis was extended to a signal portion of 10 milliseconds. The presence of the swept interference clearly emerges from Figure 5, that can be easily used for the estimation of the interference instantaneous frequency. The information extracted from the spectrogram in Figure 5 can then be easily used for different excision algorithms [4, 7]. In Figure 6, the power spectral density (PSD) of the input signal has been reported. In Figure 6(a), the PSD has been estimated by considering the downconverted GPS signal with a sampling

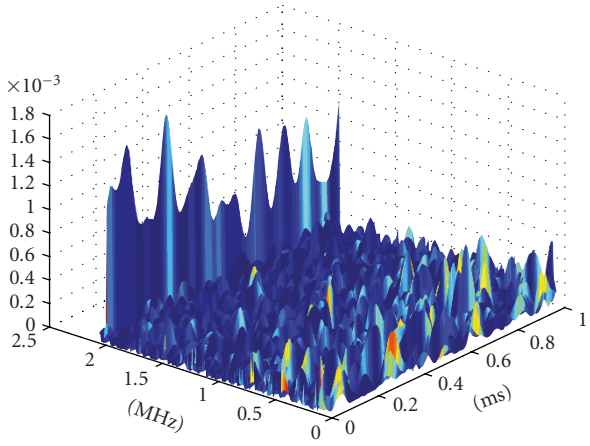

FIGURE 7: Spectrogram of a CWI. The input signal has been collected by using the NordNav R30 front-end on the hill of Superga, Torino (Italy). The spectrogram has been evaluated by using the modified parallel acquisition scheme in time domain.

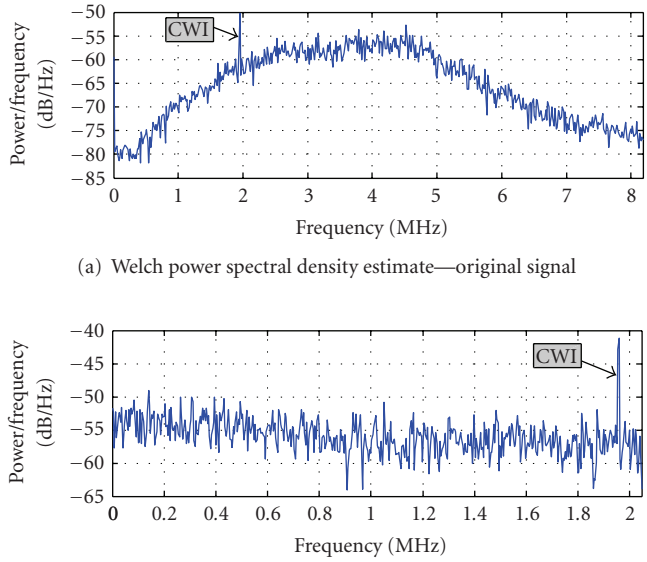

FIGURE 8: Power spectral density estimates of the input signal used for the evaluation of the spectrogram in Figure 7. (a) PSD of the original signal, sampling frequency $f_s = 16.3676$ MHz. (b) PSD of the downsampled signal, sampling frequency $f_s = 4.0919$ MHz.

frequency $f_s = 16.3676$ MHz: in this case the interference spectral components clearly emerge, although they are spread over a band of more than 1 MHz. Downsampling makes the PSD of the input signal fold, producing a noise term that is almost white and aliasing the interfering signal at a different frequency. The presence of a white noise term makes a wideband interfering signal hardly detectable in the frequency domain. In Figure 6(b), the PSD of the signal used for the evaluation of the spectrogram in Figure 5 has been depicted. In this case, the interference cannot be easily localized in the frequency domain, proving the effectiveness of TF detection techniques versus traditional pure frequency detection methods.

In Figures 7 and 8, the spectrogram and the PSDs of the signal observed at the hill of Superga are depicted. In this case, the CWI is well localized in both TF and frequency domains. The spectrogram has been evaluated by using the modified parallel acquisition scheme in time domain, with a Hamming window of duration $T_w = N/8$. As for the first case, the Doppler step has been set to 10 kHz and the number of Doppler bins was $K = 201$.

5.2. Simulated data

In order to further test the modified acquisition scheme for TF interference detection, the case of pulsed interference has been considered. In particular, GPS signals in presence of pulsed interference have been simulated and analyzed with the modified parallel acquisition scheme in time domain. The same sampling frequency and intermediate frequency of Table 1 have been adopted for the simulation. Pulsed interference can be generated by different sources such as distance measuring equipment (DME) and tactical airborne navigation (TACAN) [25] that are currently used for distance measuring and for civil and military airborne landing. The pulsed interference has been simulated as a pair of modulated Gaussian impulses [25]. The results of the test have been depicted in Figure 9, where the case of impulses with a peak

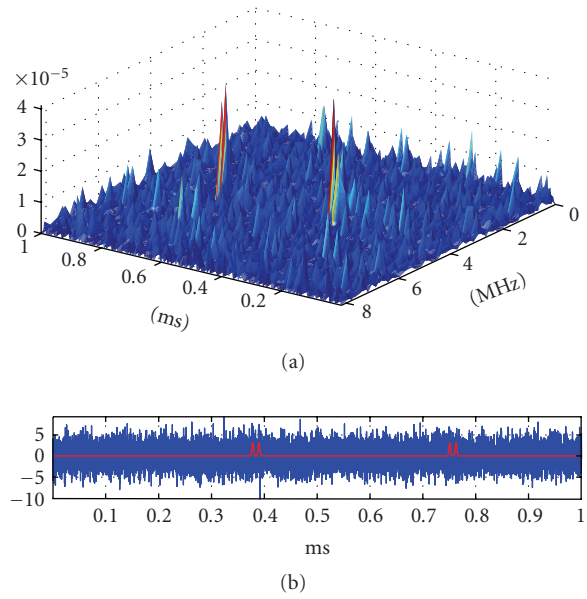

FIGURE 9: Spectrogram and time domain representation of a simulated GPS signal corrupted by pulsed interference. The spectrogram has been evaluated by using the modified parallel acquisition scheme in time domain.

power equal to the noise variance has been considered. In the bottom part of Figure 9, the time representation of the input signal has been depicted. The light line represents the envelope of the pulsed interference that cannot be directly identified from the time representation of the input signal.

When the TF representation is considered, the pulsed interference is clearly identified, allowing the efficient excision of the disturbing signal. The spectrogram of Figure 9 has been evaluated by using the modified parallel acquisition scheme in time domain, with a Hamming window of duration $T_w = N/64$. The Doppler step has been set to 200 kHz and the number of Doppler bins was $K = 41$.

6. CONCLUSIONS

In this paper, the problem of effectively implementing TF algorithms in GNSS receivers has been addressed. More specifically, a modified acquisition algorithm has been proposed in order to efficiently reuse the hardware already available in a GNSS receiver for TF applications. The proposed method is suitable for all acquisition schemes and its effectiveness has been proven by means of analysis on real data and by simulations.

ACKNOWLEDGMENTS

The authors would like to thank Laura Camoriano and Tereza Cristina Gondim Corsini for their support during data collection.

REFERENCES

[1] R. J. Landry and A. Renard, "Analysis of potential interference sources and assessment of present solutions for GPS/GNSS receivers," in *Proceedings of the 4th Saint Petersburg International Conference on Integrated Navigation Systems (INS '97)*, Saint Petersburg, Russia, May 1997.

[2] L. Cohen, *Time Frequency Analysis: Theory and Applications*, Prentice Hall PTR, Englewood Cliffs, NJ, USA, 1994.

[3] M. V. Tazebay and A. N. Akansu, "A performance analysis of interference excision techniques in direct sequence spread spectrum communications," *IEEE Transactions on Signal Processing*, vol. 46, no. 9, pp. 2530–2535, 1998.

[4] C. Wang and M. G. Amin, "Performance analysis of instantaneous frequency-based interference excision techniques in spread spectrum communications," *IEEE Transactions on Signal Processing*, vol. 46, no. 1, pp. 70–82, 1998.

[5] M. G. Amin, C. Wang, and A. R. Lindsey, "Optimum interference excision in spread spectrum communications using open-loop adaptive filters," *IEEE Transactions on Signal Processing*, vol. 47, no. 7, pp. 1966–1976, 1999.

[6] X. Ouyang and M. G. Amin, "Short-time Fourier transform receiver for nonstationary interference excision in direct sequence spread spectrum communications," *IEEE Transactions on Signal Processing*, vol. 49, no. 4, pp. 851–863, 2001.

[7] S. Barbarossa and A. Scaglione, "Adaptive time-varying cancellation of wideband interferences in spread-spectrum communications based on time-frequency distributions," *IEEE Transactions on Signal Processing*, vol. 47, no. 4, pp. 957–965, 1999.

[8] S. R. Lach, M. G. Amin, and A. R. Lindsey, "Broadband interference excision for software-radio spread-spectrum communications using time-frequency distribution synthesis," *IEEE Journal on Selected Areas in Communications*, vol. 17, no. 4, pp. 704–714, 1999.

[9] E. D. Kaplan and C. Hegarty, Eds., *Understanding GPS: Principles and Applications*, Artech House, Boston, Mass, USA, 2nd edition, 2005.

[10] P. Misra and P. Enge, *Global Positioning System, Signals, Measurements and Performance*, Ganga-Jamuna Press, Lincoln, Mass, USA, 2006.

[11] R. J. Landry, V. Calmettes, and M. Bousquet, "Impact of interference on a generic GPS receiver and assessment of mitigation techniques," in *Proceedings of the 5th IEEE International Symposium on Spread Spectrum Techniques and Applications (ISSSTA '98)*, vol. 1, pp. 87–91, Sun City, South Africa, September 1998.

[12] J. A. Young and J. S. Lehnert, "Analysis of DFT-based frequency excision algorithms for direct-sequence spread-spectrum communications," *IEEE Transactions on Communications*, vol. 46, no. 8, pp. 1076–1087, 1998.

[13] Z. Yimin, M. G. Amin, and A. R. Lindsey, "Anti-jamming GPS receivers based on bilinear signal distributions," in *Proceedings of the IEEE Military Communications Conference (MILCOM '01)*, vol. 2, pp. 1070–1074, McLean, Va, USA, October 2001.

[14] C. Yang, "Method and device for rapidly extracting time and frequency parameters from high dynamic direct sequence spread spectrum radio signals under interference," US patent 6407699, June 2002.

[15] D. J. R. van Nee and A. J. R. M. Coenen, "New fast GPS code-acquisition technique using FFT," *Electronics Letters*, vol. 27, no. 2, pp. 158–160, 1991.

[16] F. J. Harris, "On the use of windows for harmonic analysis with the discrete Fourier transform," *Proceedings of the IEEE*, vol. 66, no. 1, pp. 51–83, 1978.

[17] Z. Weihua and J. Tranquilla, "Modeling and analysis for the GPS pseudo-range observable," *IEEE Transactions on Aerospace and Electronic Systems*, vol. 31, no. 2, pp. 739–751, 1995.

[18] J. B.-Y. Tsui, *Fundamentals of Global Positioning System Receivers: A Software Approach*, Wiley-Interscience, New York, NY, USA, 2000.

[19] F. Hlawatsch and G. F. Boudreaux-Bartels, "Linear and quadratic time-frequency signal representations," *IEEE Signal Processing Magazine*, vol. 9, no. 2, pp. 21–67, 1992.

[20] M. G. Amin and K. Di Feng, "Short-time Fourier transforms using cascade filter structures," *IEEE Transactions on Circuits and Systems II*, vol. 42, no. 10, pp. 631–641, 1995.

[21] D. Akopian, "Fast FFT based GPS satellite acquisition methods," *IEE Proceedings: Radar, Sonar and Navigation*, vol. 152, no. 4, pp. 277–286, 2005.

[22] P. Misra and P. Enge, *Global Positioning System: Signals, Measurements and Performance*, Ganga-Jamuna Press, Lincoln, Mass, USA, 2006.

[23] J. Proakis, *Digital Communications*, McGraw-Hill, New York, NY, USA, 4th edition, 2000.

[24] *NordNav-R30 Package*, NordNav Technologies, 2004, http://www.navtechgps.com/pdf/r30.pdf.

[25] F. Bastide, E. Chatre, C. Macabiau, and B. Roturier, "GPS L5 and Galileo E5a/E5b signal-to-noise density ratio degradation due to DME/TACAN signals: simulations and theoretical derivation," in *Proceedings of the ION/NTM National Technical Meeting*, pp. 1049–1062, San Diego, Calif, USA, January 2004.